

AD _____

Award Number: W81XWH-06-C-0360

TITLE: Discovery of Novel Virulence Factors of Biothreat Agents: Validation of the Phosphoproteome-Based Approach

PRINCIPAL INVESTIGATOR: Charles L. Bailey, Ph.D.
Monique L. van Hoek, Ph.D.

CONTRACTING ORGANIZATION: George Mason University
Fairfax, VA 22030

REPORT DATE: June 2007

TYPE OF REPORT: Annual

PREPARED FOR: U.S. Army Medical Research and Materiel Command
Fort Detrick, Maryland 21702-5012

DISTRIBUTION STATEMENT: Approved for Public Release;
Distribution Unlimited

The views, opinions and/or findings contained in this report are those of the author(s) and should not be construed as an official Department of the Army position, policy or decision unless so designated by other documentation.

REPORT DOCUMENTATION PAGE				Form Approved OMB No. 0704-0188	
Public reporting burden for this collection of information is estimated to average 1 hour per response, including the time for reviewing instructions, searching existing data sources, gathering and maintaining the data needed, and completing and reviewing this collection of information. Send comments regarding this burden estimate or any other aspect of this collection of information, including suggestions for reducing this burden to Department of Defense, Washington Headquarters Services, Directorate for Information Operations and Reports (0704-0188), 1215 Jefferson Davis Highway, Suite 1204, Arlington, VA 22202-4302. Respondents should be aware that notwithstanding any other provision of law, no person shall be subject to any penalty for failing to comply with a collection of information if it does not display a currently valid OMB control number. PLEASE DO NOT RETURN YOUR FORM TO THE ABOVE ADDRESS.					
1. REPORT DATE (DD-MM-YYYY) 01-06-2007		2. REPORT TYPE Annual		3. DATES COVERED (From - To) 1 Jun 2006 – 31 May 2007	
4. TITLE AND SUBTITLE Discovery of Novel Virulence Factors of Biothreat Agents: Validation of the Phosphoproteome-Based Approach				5a. CONTRACT NUMBER W81XWH-06-C-0360	
				5b. GRANT NUMBER	
				5c. PROGRAM ELEMENT NUMBER	
6. AUTHOR(S) Charles L. Bailey, Ph.D. and Monique L. van Hoek, Ph.D. E-Mail: ddonaho@gmu.edu				5d. PROJECT NUMBER	
				5e. TASK NUMBER	
				5f. WORK UNIT NUMBER	
7. PERFORMING ORGANIZATION NAME(S) AND ADDRESS(ES) George Mason University Fairfax, VA 22030				8. PERFORMING ORGANIZATION REPORT NUMBER	
9. SPONSORING / MONITORING AGENCY NAME(S) AND ADDRESS(ES) U.S. Army Medical Research and Materiel Command Fort Detrick, Maryland 21702-5012				10. SPONSOR/MONITOR'S ACRONYM(S)	
				11. SPONSOR/MONITOR'S REPORT NUMBER(S)	
12. DISTRIBUTION / AVAILABILITY STATEMENT Approved for Public Release; Distribution Unlimited					
13. SUPPLEMENTARY NOTES					
14. ABSTRACT See next page.					
15. SUBJECT TERMS No subject terms provided.					
16. SECURITY CLASSIFICATION OF:			17. LIMITATION OF ABSTRACT	18. NUMBER OF PAGES	19a. NAME OF RESPONSIBLE PERSON
a. REPORT	b. ABSTRACT	c. THIS PAGE			USAMRMC
U	U	U	UU	31	19b. TELEPHONE NUMBER (include area code)

Abstract

Purpose and Scope: We are developing a novel application of Reverse Phase Protein Microarrays (RPMA) technology to the study of biothreat organisms. The power of this technology to survey the phosphorylation status of multiple proteins simultaneously enables us to map the host cell response to infection with multiple strains and species of *Francisella* as well as to begin to dissect which individual factors or proteins are contributing to the complex signals generated during infection, and thereby perhaps also to virulence. We will demonstrate the utility of this technology to examine host responses to bacterial infection, host responses to extracellular macromolecules, and host responses to individual proteins applied either extracellularly or intracellularly to the host cell. We will also compare different strains and species of *Francisella* using RPMA to elucidate the molecular differences in host response to the strains. Furthermore, we will begin to establish a model of how to use RPMA to screen a genome-worth of open reading frames (ORFs) for potential virulence factors (VFs) by identifying those factors with an effect on host cell signaling pathways.

Results: In the first year of this project, we have successfully performed Reverse Phase MicroArray (RPMA) of *Francisella novicida* in J774A.1 murine macrophages. In so doing, we have performed detailed RPMA analysis of the following proteins over a time course of infection: NFkB, IKBa, p38 MAPK, JNK, Src, Lck, Caspase 9, Caspase 3, Bcl2, and Bax, among others. We have found time-specific changes in these proteins during infection representing the Toll-like receptor pathway, the AKT pathway and the apoptotic pathway. We have begun a comparison and correlation of RPMA results to published results of the effects of *Francisella* infection on host cells, the results of which will be presented in a poster and are being prepared as a manuscript. We have also made significant progress on cloning known virulence factors of *Francisella* to be used in testing our hypothesis. We have successfully expressed tagged iglC protein in a bacterial expression vector and are purifying this protein for further study. In addition, we have confirmed by RT-PCR the mammalian expression of tagged iglC protein.

Significance: We have demonstrated that RPMA can be used to rapidly characterize the effect of bacterial infection on host cells by examining alterations in phosphorylation of multiple signaling pathway proteins. Through the ability of the protein array technology to measure hundreds of signaling events at once, in effect providing a real-time molecular network map, RPMA analysis will allow us to discover the full complement of signaling systems that could serve as new targets for intervention and therapy. The comparative analysis of signaling profiles will further aid us in understanding the key elements of virulence and pathogenesis, a critical step along the path to development of vaccines and therapeutics.

Table of Contents

	<u>Page</u>
Introduction.....	5
Body.....	6
Key Research Accomplishments.....	28
Reportable Outcomes.....	28
Conclusion.....	29
References.....	29
Appendices.....	30

INTRODUCTION:

Reverse Phase Protein Microarrays (RPMA) are a powerful new technology that can be applied to the post-genomic era of microbial pathogenesis studies. We are developing a novel application of RPMA technology to the study of biothreat organisms – to rapidly characterize the effect of bacterial infection on host cells by examining alterations in phosphorylation of multiple signaling pathway proteins. The power of this technology to survey the phosphorylation status of multiple proteins simultaneously enables us to map the host cell response to infection with multiple strains and species of *Francisella* as well as to begin to dissect which individual factors or proteins are contributing to the complex signals generated during infection, and thereby perhaps also contributing to virulence. We will demonstrate the utility of this technology to examine host responses to bacterial infection, host responses to extracellular macromolecules, and host responses to individual proteins applied either extracellularly or intracellularly to the host cell. We will also compare different strains and species of *Francisella* using RPMA to elucidate the molecular differences in host response to the strains. Furthermore, we will begin to establish a model of how to use RPMA to screen a genome-worth of open reading frames (ORFs) for potential virulence factors (VFs) by identifying those factors with an effect on host cell signaling pathways.

BODY:

Task 1: Validation of Reverse Phase Protein Microarray (RPMA) technology

NOTE: For purposes of explanation, Task 1.7 will be discussed first.

Task 1.7: Generate the phosphoactivation map of *Francisella tularensis novicida* infected J774A.1 macrophage cells. Compare the phosphoactivation profiles generated to published results with other *Francisella* strains in J774A.1 cells for validation.

A. Two-hour preinfection protocol:

Following the protocol outlined in the proposal, an infection time course in J774A.1 cells was performed using *F. novicida*. The cells were pre-infected for 2 hours, and then proteins were harvested from infected cells in TPER buffer (Pierce, Madison, WI) plus protease inhibitors at different time points from 0 min, 5 min, 15 min, 30 min, 1 hour, 2 hours, 4 hours, 6 hours, 8 hours. Uninfected cells were harvested at time 0 and 8 hrs as controls. Time zero (0) was the first time point collected after the 2 hour preincubation. The lysates are then spotted onto a microarray slide and subjected to automated Western Blotting with phosphor-specific antibodies to detect the amount of phosphoprotein present at each time point. Serial dilutions within each lysate sample are also spotted onto the slide to ensure that detection will be within the linear range for each sample. Spots are developed with colorimetric detection and will be scanned for pixel intensity to measure the amount of phosphoprotein in each spot. Total protein is determined by Sypro staining (protein stain) one slide of spotted lysates. Controls include A431 lysates with and without EGF, which should contain highly phosphorylated proteins, as well as a series of control phosphopeptides. Sample slides prepared for this experiment are illustrated in Figure 1, and the slide-map is presented in Figure 1-A.

Figure 1: A: RPMA Slide Schematic. The series of dilutions of each lysate is seen by the 6 dots of decreasing intensity.

Uninfected 0 hr (3 rows of 6 dots)	Uninfected 8 hr (3 rows of 6 dots)	T=0 (3 rows of 6 dots)	A431 Lysate (3 rows of 6 dots)	A431 Lysate + EGF (3 rows of 6 dots)
T=5' (3 rows of 6 dots)	T=15' (3 rows of 6 dots)	T=30' (3 rows of 6 dots)	Phosphopeptide Controls (3 rows of 6 dots)	EMPTY
T=60' (3 rows of 6 dots)	T=2 hr (3 rows of 6 dots)	T=4 hr (3 rows of 6 dots)	EMPTY	EMPTY
T=6 hr (3 rows of 6 dots)	T=8 hr (3 rows of 6 dots)	EMPTY	EMPTY	EMPTY

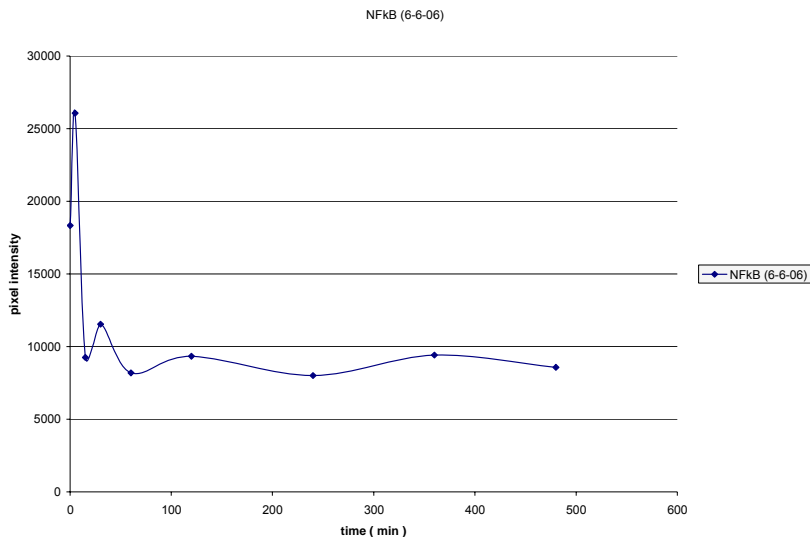
Figure 1-B: RPMA analysis using phospho-JNK, phospho-NFKB, phospho-IKB-alpha antibodies to probe a time-course of *Francisella* infected J774A.2 macrophages. Please refer to schematic in Figure 1-A



After the pixel intensity of each spot is measured, and normalized for total protein and linearity using MicroVigene™ program to measure and calculate the relative values, it is possible to

generate a graphical representation of the change in phosphorylation of each protein over the time course of infection. Two such graphs are presented in Figure 2 and 3 below. **Figure 2** illustrates the change for phospho-NFkB over this infection time course, and **Figure 3** illustrates the changes for phospho-c-Src over this infection time course. These results illustrate that the phosphorylation status of these two proteins changes over the time course of being infected by *Francisella novicida*.

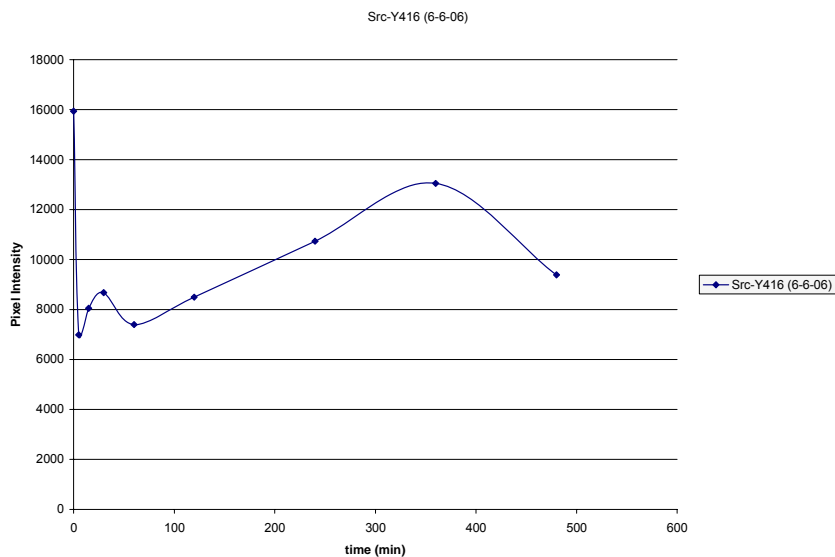
Figure 2: Graphic representation of RPPMA results of NFkB-ser536. NFkB transcription factor



is a protein dimer which regulates the expression of a large number of genes. NFkB itself is regulated through phosphorylation on a number of different amino acid residues. The monomer p65 can be phosphorylated on residue serine 536 (S536) after physiological induction with pro-inflammatory stimuli (14, 15). Results from RPPMA using the phospho-specific NFkB antibody show an increase in phosphorylation at S536 in the short time periods (less than one hour)

after pre-infection with *F. tularensis*. This increase peaks at 15 minutes, showing a greater than 3-fold increase in phosphorylation. These data suggest NFkB changes in activation after infection.

Figure 3: Graphic representation of RPPMA results of c-SrcY416. c-Src is a protein tyrosine



kinase which regulates many signal transduction pathways in eukaryotic cells. C-Src itself is regulated through phosphorylation on tyrosine residue 416. Results from RPPMA using the phospho-specific c-Src antibody show early high levels, a decrease at short time periods (less than one hour) and a slow increase in phosphorylation at Y416 in the long time periods after pre-infection with *F. tularensis*. These data suggest c-Src changes in

activation after infection.

B. Real time Infection Protocol: No preinfection.

We adapted the protocol as originally outlined in the proposal in order to accommodate examining the host cell signaling at much earlier time-points, and we eliminated the two hour preinfection that was done in the initial studies. In this regard, we are considering the bacteria to be a “signaling input” in an analogous fashion to adding EGF to a cell, for example. Thus, the previously obtained data still speaks to the later events during *Francisella* infection (between 3-24 hours), but will not reflect signaling changes that occur within the first 2 hours of infection. Using the new protocol, an infection time course in J774A.1 cells was performed using *F. novicida* as the “signaling input”. Briefly, the cells were planted 24 hours prior to the infection, the bacteria were applied to the cells with centrifugation at an MOI of 500, and then proteins were harvested from infected cells in TPER buffer (Pierce, Madison, WI) plus protease and phosphatase inhibitors at different time points from 5 min, 15 min, 30 min, 1 hour, 2 hours, 4 hours, and 6 hours. Uninfected cells were harvested at time 0 and 8 hrs as controls. Time zero (0) is now the equivalent to uninfected cells.

Figure 4a: RPMA of phospho-NF-kB

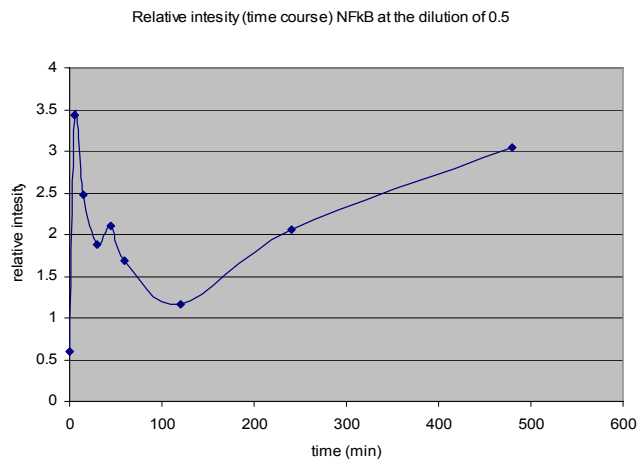


Figure 4b: RPMA of phospho-p38

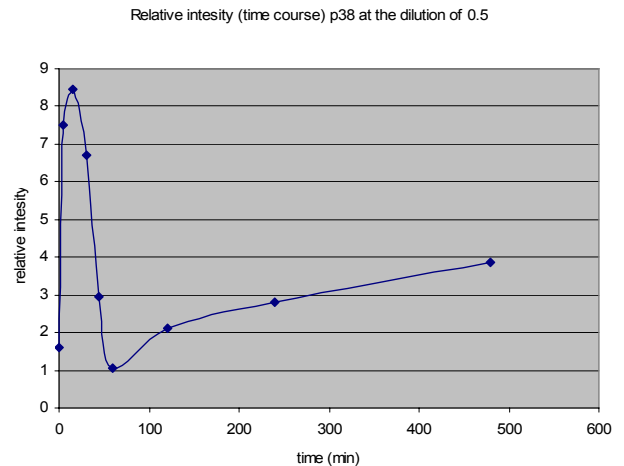


Figure 4c: RPMA of BCL

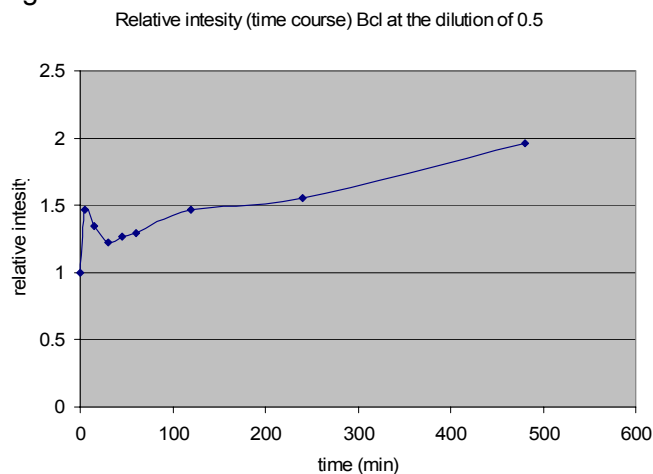


Figure 4d: RPMA of FAK

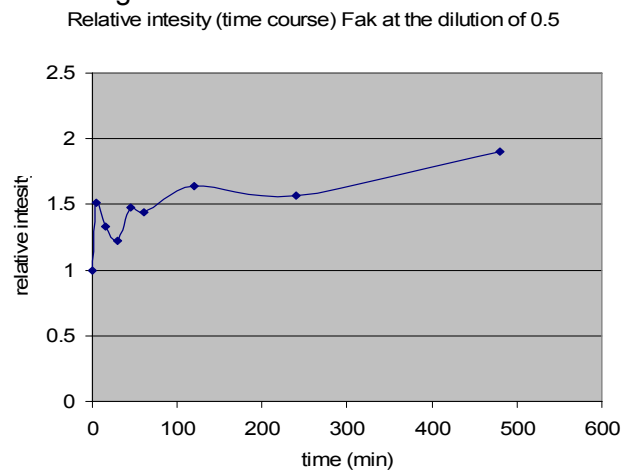


Figure 4: Graphical representation of changes in the phosphoproteome of J774A.1 macrophages following *F. novicida* infection for critical phosphoproteins. These four graphs represent some of the different patterns of response seen for various critical phosphoproteins in response to *Francisella* infection. Some signals peak at 5 or 15 minutes, while other have a slower increase over the infection time. Other antibodies have been tested, for which we are still analyzing and interpreting the results include Bad, Bax, Bcl, Caspase 3, Caspase 9, FAK, IκB, Jnk, Lck, and Src.

Our second goal for Q3 was to continue our work to verify and support the RPMA results with Western Blots of the same experiments and the same antibodies. **Figure 5** illustrates such a blot for NF-κB for the RPMA lysate studied in this experiment. This data shows that the Total amount of NF-κB protein in the lysates is not changing over the time of the infection, but the amount of the phosphorylation of NF-κB is changing at the early time points, confirming our findings from RPMA.

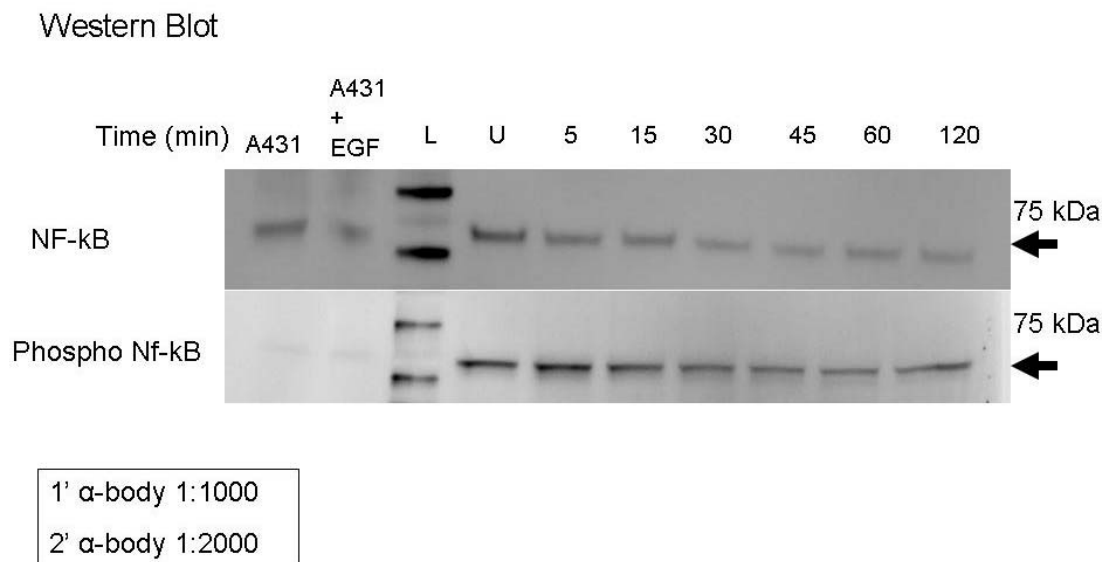


Figure 5: Western blot of NF-κB (1-19-07) whole cell lysate in infected J774A.1 cells by *Francisella novicida*. No pre-infection. Time was then calculated by the point when the gentamycin solution 2 was added. All cells were lysed at the same time. Lane 1 is A431 cell lysate provided by BD Bioscience (#611447) and was used as a standard control. Lane 2 is A431 + EGF cell lyaste provided by BD Bioscience (#611448) and was used as a standard control for total phosphorylated protein. Lane 3 is Sea Blue Plus 2 and Magic Mark XP western ladder. Lane 4 is non-infected control J774A.1 cells. Lane 5 is J774A.1 cells infected with *F. novicida* when time = 0. Lane 6 is J774A.1 cells infected with *F. novicida* when time = 15 minutes. Lane 7 is J774A.1 cells infected with *F. novicida* when time = 30 minutes. Lane 8 is J774A.1 cells infected with *F. novicida* when time = 1 hour. Lane 9 is J774A.1 cells infected with *F. novicida* when time = 2 hours. Lane 10 is is J774A.1 cells infected with *F. novicida* when time = 4 hours. Ponceau S staining of the blot was performed to confirm that equal total protein was loaded in each lane.

We had performed a subsequent infection which we discovered to have been an experimental failure, proving that our experimental approach has strong internal controls. In this particular case, in adapting the new protocol, the bacteria were applied at an MOI of 500, but

were not centrifuged to encourage contact with the mammalian cells. Following the infection at each time point, lysates were collected as before for protein analysis, RPMA and Western Blotting. In a separate plate, the same protocol was followed for early timepoints and the cells were lysed and plated out on chocolate agar to confirm the infection. It turns out that incubating the cells with the bacteria in the absence of centrifugation does not lead to an adequate infection at the early timepoints, as no colonies were obtained at those timepoints. Further, when a Western Blot was performed for phospho-AKT of these lysates, no change in phosphorylation was seen over the time, further supporting that there was no infection in this particular case. RPMA was not performed on these lysates. There are two recent reports in the literature of AKT being phosphorylated following *Francisella* infection (1, 13), which was what we would have expected if the infection had been successful. Thus, we are pleased that our experimental design is successful in revealing interesting changes in key regulatory molecules following *Francisella* infection, and we are further pleased that our experimental design is robust enough to catch experimental failures, as described here.

C. Total Protein Analysis of RPMA lysates on slides:

Following the protocol outlined in the proposal, an infection time course in J774A.1 cells was performed using *F. novicida* as reported in the Q1 report. Briefly, the cells were pre-infected for 2 hours, and then proteins were harvested from infected cells in TPER buffer (Pierce, Madison, WI) plus protease inhibitors at different time points from 0 min, 5 min, 15 min, 30 min, 1 hour, 2 hours, 4 hours, 6 hours, 8 hours. Uninfected cells were harvested at time 0 and 8 hrs as controls. Time zero (0) was the first time point collected after the 2 hour preinfection. The lysates were then spotted onto a microarray slide and subjected to automated Western Blotting with phospho-specific antibodies to detect the amount of phosphoprotein present at each time point. Serial dilutions within each lysate sample were also spotted onto the slide to ensure that detection was within the linear range for each sample. Spots were developed with colorimetric detection and will be scanned for pixel intensity to measure the amount of phosphoprotein in each spot. Total protein was determined by Sypro staining (protein stain) one slide of spotted lysates. Controls included A431 lysates with EGF, which should contain highly phosphorylated proteins, A431 lysates without EGF, which should have lower levels of phosphorylated proteins, as well as a series of control phosphopeptides.

When the spots on the microarray slide are analyzed, the first step is a parsing of the data to eliminate any spots that may lie outside of the linear range of the detection assay. This parsing can be done within a data analysis program such as MicroVigene™ or manually, by graphing the pixel intensity of staining of each spot versus the dilution curve. Although the MicroVigene program facilitates the final data analysis once outlier spots have been manually selected for elimination, it does so in a pre-programmed manner that is not clearly explained nor can it be controlled by the user. In order to attempt to parse the data in a fair way without using the MicroVigene program, Dr. Yuka Taylor, who is a mathematician working part-time in our lab, has agreed to perform data analysis on the scanned results of the slides presented in the last report. In particular, we focused our attention on the Total Protein Slide and the phospho-NFkB slide. Following the elimination of outlier spots, a line with a strong R^2 can be obtained from plotting the dilution factor versus the pixel intensity. By performing this analysis on each data timepoint for the Total Protein Slide, we can then compare these results to the antibody results and find the relative amount of change for the phosphoantibody RPMA. As an example of this analysis, **Figure 6** illustrates a dilution curve for the Total Protein staining of the “360 minute” sample, plotting the pixel intensity of the protein stain versus the dilution factor for each spot.

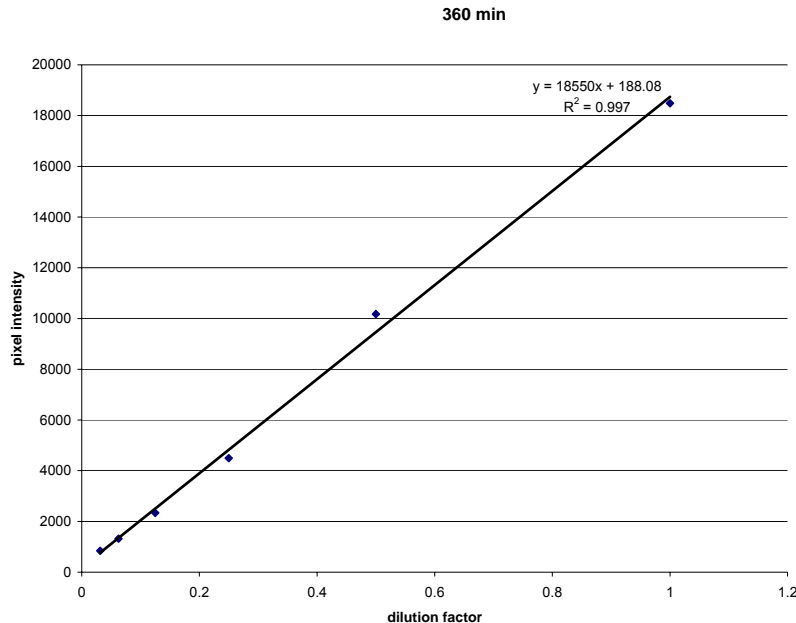


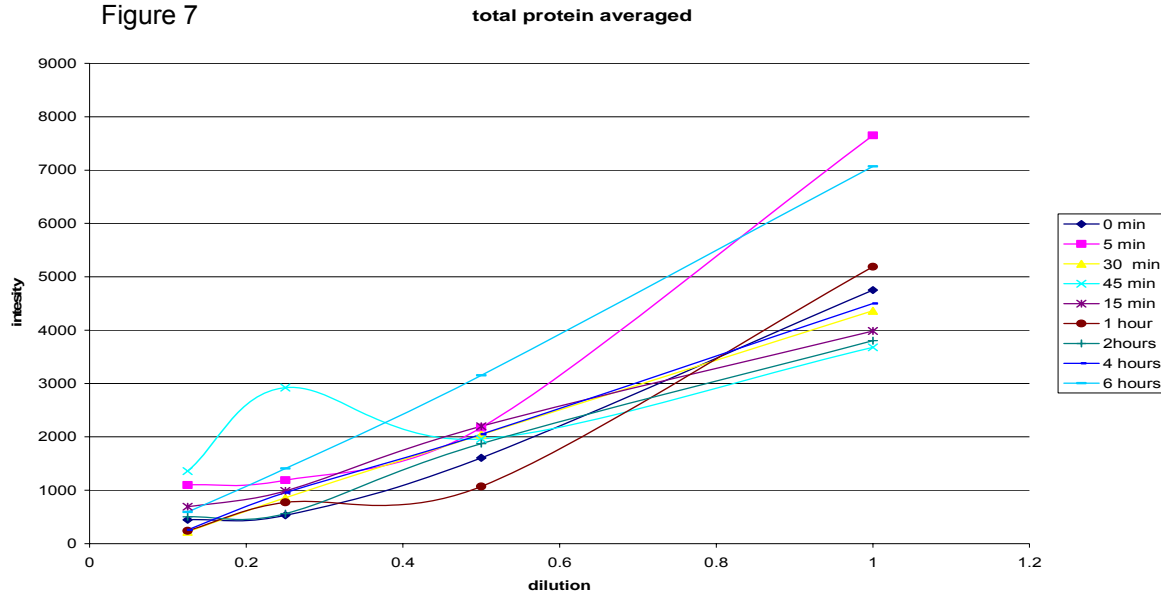
Figure 6: Plot of the pixel intensity of spots versus the dilution factor to determine the linearity of the data. In this case, the data obtained at 360 minutes of infection are illustrated, after the outlier spots were eliminated. Similar analyses were performed for each time point, but are not shown here. Linearity of the data is revealed by the R^2 measurement being close to 1 (here, $R^2 = 0.997$).

From this analysis, we have evidence indicating several important factors that will lead to more optimal experimental design. The first factor which we have determined is that even though the protocol does not require the measurement of protein concentration of each individual well at each time point of infection, the protein levels between all the wells were fairly constant, within one standard deviation of each other. Further, we determined that duplicate sample spotting as called for in the original protocol are too limiting in terms of data analysis (after non-linear spots are discarded) and that much stronger statistical correlations can be drawn if triplicate samples are spotted for each dilution curve. This changes the slide layouts and the total number of samples that can be analyzed per slide, but probably improves the data overall.

Analysis of Total protein levels using the Real Time Infection Protocol.

Following infection of J774A.1 murine macrophages with *Francisella tularensis novicida*, cell lysates were collected at 5, 15, 30, 45, 60, 120, 240, and 480 minutes with **no preinfection**. The total protein of each lysate was determined. Each dilution point was averaged and then graphed (Figure 7). The 0.25 concentration was then picked to analyze all other antibodies as it appears to contain the least variance over the time course. (The 45 minute time point was thrown out at this spot because of irregularities in the Sypro stain on the slide at this time point.). Antibody intensity was calculated by subtracting the net average intensity at a time point from the net negative intensity from the corresponding time point. Each time point at the 0.25 dilution was then graphed together to give the overall relative changes in phosphorylation signaling of that antibody over time. From Figure 7 it can be observed that all the samples had similar protein amounts.

Figure 7



Task 1.1: Generate the phosphoactivation map of *Francisella* LVS infected J774A.1 macrophage cells.

New stock of *Francisella tularensis* LVS was obtained from BEI Resources (ATCC) to ensure the consistency with the banked strains. Infection time courses have been prepared with *Francisella* LVS and J774A.1 macrophages. RPMA assays will be performed as soon as slides are available from the manufacturer.

Task 1.2: Generate the phosphoactivation map of *Francisella* LVS Lipopolysaccharide (LPS) treated J774A.1 macrophage cells.

Work on this task will begin in Year 2.

Task 1.3: Compare the phosphoactivation profiles generated by RPMA to published results in J774A.1 cells and provide conclusions regarding the validation of RPMA technology.

Multiple pathways are activated during bacterial infections of macrophage. During the first few minutes of infection these pathways focus on the production proteins that will regulate pro-inflammatory cytokines, chemotaxis cytokines, apoptosis, and cytoskeleton rearrangement. The production of these proteins and events will eventually elicit a total innate immune system response. However *Francisella* bacteria have found ways to evade and/or stop the proper signaling cascade activation (5). *Francisella* is an intracellular pathogen that enters the cell through an unknown mechanism. Once in the cell, *Francisella* is encapsulated in a phagosome. Between 2-4 hours after the initial infection *Francisella* escapes the phagosome and proceeds to replicate in the hosts cytosol (2). Previous studies have demonstrated that *Francisella* inhibits the release of pro-inflammatory cytokines such as TNF-alpha, IL-1, IL-12, and IL-8 hampering the ability of the innate immune system to respond to infection (16). Also, there is an increase of IL-10 seen during *Francisella* infection. IL-10 is an anti-inflammatory cytokine that further decreases the innate immune system response (16). The lack of proper cytokine

production might be caused by *Francisella*'s ability to block the TLR pathways, AKT pathways, and the apoptosis pathways, further impeding the innate immune response. Interestingly, *Francisella* does not employ the secretion systems, such as type III or type IV secretion systems, that are commonly found in pathogenic bacteria (1), nor does it produce toxins that could explain its ability to block cell signaling pathways.

Through the use of RPMA we will be able to gain a better understanding of what, where, and how pathways are blocked during *Francisella* infection. This information is critical in unlocking how *Francisella* evades the immune system. For antibody selection in the RPMA, we will focus on phosphoproteins within three main pathways: the toll-like receptor (TLR) pathway, AKT pathway and apoptosis pathway (8, 13, 14). Signaling through these pathways have previously been shown to be impacted during an infection with *Francisella* and therefore a detailed molecular analysis using RPMA could provide insight into how *Francisella* is able to hamper proper cell signaling.

1) TLR Pathway:

The TLR pathways have been extensively studied in other organisms. TLRs are transmembrane pattern recognition receptors (PRR) that are part of the interleukin-1 receptor (IL-1R) super family. TLRs are able to recognize highly conserved regions on pathogens known as pattern-associated molecules proteins (PAMPs). There are ten TLRs in the human genome and can be located on the cell membrane as in the case of TLR2 and 4 or can be located in the phagosome membrane like TLR3 (6, 9, 11). TLR4, for example, is capable of recognizing lipopolysaccharide (LPS) which is associated with gram negative bacteria's cell membrane. For signaling to occur through TLR4 the LPS must first bind to LPS binding protein (LBP) which binds to CD14 (a transmembrane receptor) (3). This allows for further binding of MD-2, which causes the release of SIGIRR from TLR4. These accessory molecules bind to TLR4 allowing it to start the signal cascade. This signaling cascade is capable of activating the MyD88 dependent pathway as well as apoptosis pathway (15).

Francisella appears to disrupt multiple points along this pathway including NF- κ B, MAPK, ERK, JNK, and p38 causing a decrease in the release of TNF- α , IL-1, and IL-8, which are all needed to induce an adaptive immune response. The disruption of NF- κ B is used by multiple pathogens to reduce the immune response (3, 14, 15). At the beginning of this study we will focus on *Francisella* ability to activate NF- κ B, phosphorylation of p38, and p42/p44 MAP-Kinase, ERK, and JNK as potential sites where *Francisella* may hamper the normal signaling cascade. RPMA will help us determine where along the TLR pathway blockage/deactivation/activation occurs. This information will allow us to narrow our search down to the most likely spots of interference, and thus lead to the discovery of novel virulence factors that were previously overlooked.

2) Apoptotic pathway:

The apoptotic pathways are also of interest during *Francisella* infection. It appears that *Francisella* down regulates apoptotic pathways early in the infection process. During early infection, *Francisella* enters the phagosome. Within 2-4 hours *Francisella* escapes the phagosome and begins to replicate in the cytosol until it reaches a critical mass (2), at which point it activates apoptotic pathways. Hrska and others have shown that p38 and p44 are down regulated which cause the cell to undergo apoptosis (7). This is an interesting finding since p38 is generally thought to be anti-apoptotic. Lai et al. demonstrated that during infection with *Francisella*, macrophages begin to signal stress events and eventually leads to the apoptosis signaling cascade (8). During a 48 hour infection, the researchers observed cell detachment

and morphological changes. They also saw an increase in caspase 3 (CC3) activation, and caspase 9 (CC9) activation, both of which function to stop apoptosis (8). Recently published studies have shown that during *Francisella* infection a clear decrease in caspase 1 activation is observed (13). This is of importance because the presence of caspase 1 generally initiates apoptosis. Through the use of RPMA we hope to discover where *Francisella* works in the disruption of the apoptosis signaling cascade, as well as look at the activation of caspase 3, caspase 9, and caspase 1.

3) AKT pathway:

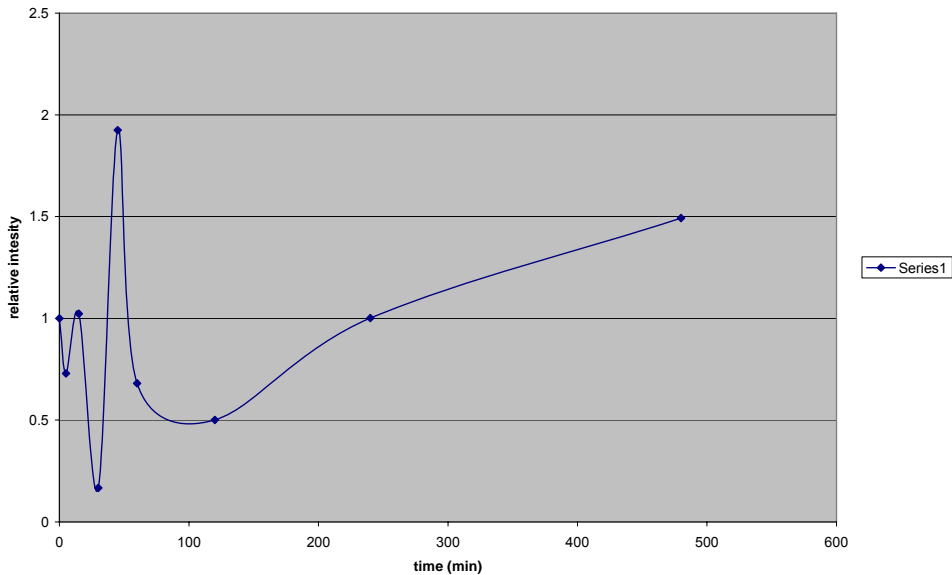
AKT is a serine/threonine kinase that is recruited to the cell membrane upon cell surface stimulation. Activation of AKT requires an association with PIP3 through AKT's PH domain, which leads to the phosphorylation of AKT. AKT is interesting because it plays a part in multiple cell signaling pathways such as cell cycle, cell survival, NF- κ B dependent gene transcription, actin remodeling, and cell migration (1, 13). Stimulation of AKT through platelet-derived growth factor (PDGF) and/or TNF- α causes AKT to phosphorylate I κ B α . I κ B α then interacts with NF- κ B, which eventually leads to cell survival (1). However, AKT in response to LPS will phosphorylate glycogen synthase kinase beta. This phosphorylation leads to glycogen synthase kinase beta inactivation, which down regulates the activity of NF- κ B. In *Francisella* infection AKT appears to negatively regulate NF- κ B. MglA is a possible virulence factor which appears to suppress AKT activity causing a decrease in IL-12, IL-6, TNF- α , and IL-1 β . Without IL-12 activation there is no natural killer response or release of IFN- γ and the infection can not be cleared (13). Interestingly, studies looking at AKT activity during *Francisella* infection saw up regulation of MAPK, ERK, p38, JNK. This correlates to what is seen when TLR pathways are examined. It is possible that these pathways are interconnected during a *Francisella* infection. RPMA allows us to look at this system more closely and identify where the changes occur in the AKT pathway.

4) RPMA results for Individual molecules:

Caspase 9 (CC9) (Figure 8) showed both up and down regulation over the infection time course, with a sharp down regulation event at 30 minutes followed by a sharp up regulation at 45 minutes. At 60 minutes we see another sharp decrease followed by a gradual increase through the end of the remainder of the experiment with the level of activated CC9 almost reaching the initial intensity as at 45 minutes. This correlates to previous reports that state that CC9 presence is an indicator of reduced apoptosis. *Francisella* infection appears after an initial decrease to cause the enhanced activation of CC9, which is an early marker for the commitment to apoptosis. Additional RPMA experiments and Western Blots will be performed in Year 2 to confirm these findings.

Figure 8

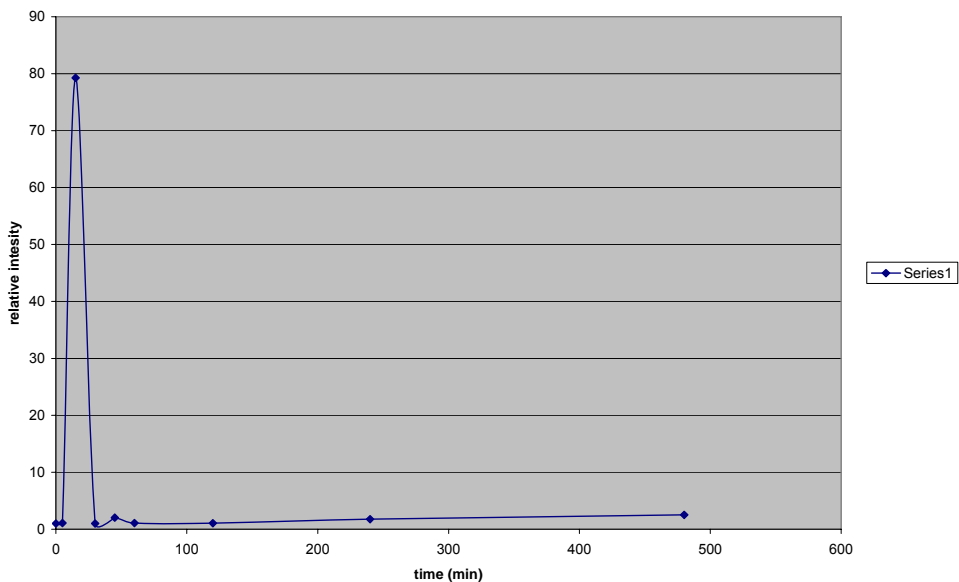
Relative intensity (time course) CC9 at the dilution of 0.25



Caspase 3 (CC3) (Figure 9) showed a different signaling pattern with the only change seen at 15 minutes. This up regulation is then followed by a marked decrease in CC3 activation. The remainder of time points shows signaling similar to what is seen in the uninfected cells. Again, like CC9, these results could indicate that the early and intense up regulation CC3 activity delays normal apoptosis during a bacterial infection. Additional RPMA experiments and Western Blots will be performed in Year 2 to confirm these findings.

Figure 9

Relative intensity (time course) CC3 at the dilution of 0.25



I κ B α (Figure 10) and NF- κ B (Figure 11) displayed a different signaling profile than those of CC9 and CC3. I κ B α has a sharp up regulation at 5 minutes followed by a decrease at 15 and 30 minutes. Again at 45 minutes there was an up regulation event. This signal gradually tapered off until 120 minutes. After 120 minutes there was a steady increase in signaling. NF-

κ B showed a similar but slower pattern, with a delay relative to I κ B α , which concurs with the requirement of activating (phosphorylating) I κ B α in order to get activation of NF- κ B. It is possible that during the early up regulation events AKT is phosphorylating I κ B α , further enhancing cell survival through I κ B α 's association with NF- κ B. The second up regulation event occurs at 45 minutes, which might correlate to the beginning stages of phagosome exit. At this point it would be important to suppress the cells apoptotic response. Additional RPMA experiments and Western Blots will be performed in Year 2 to confirm these findings.

Figure 10 Relative intensity (time course) I κ B α at the dilution of 0.25

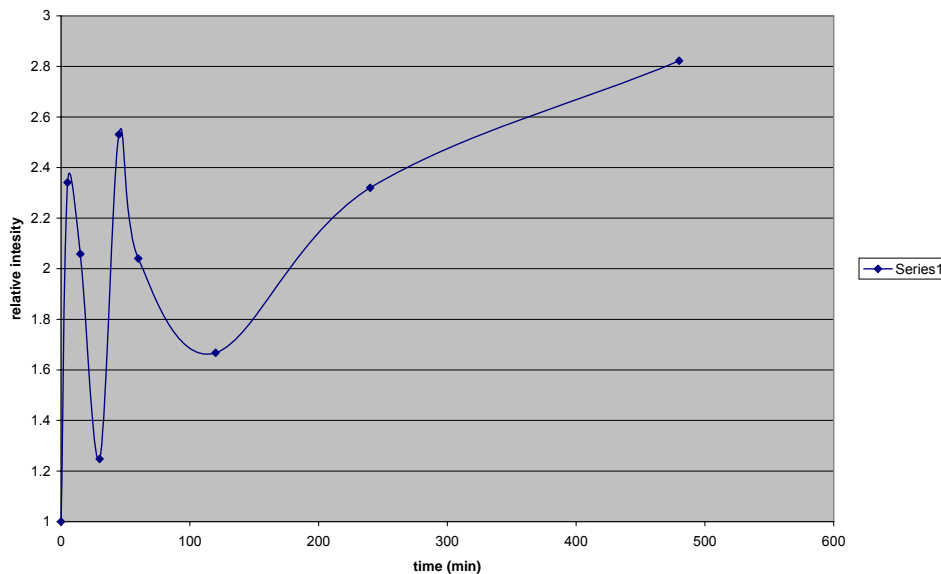
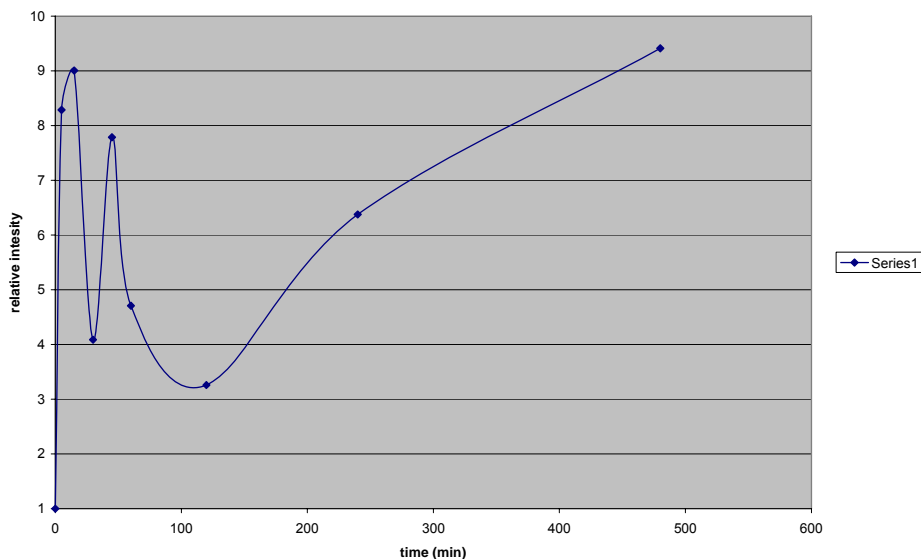
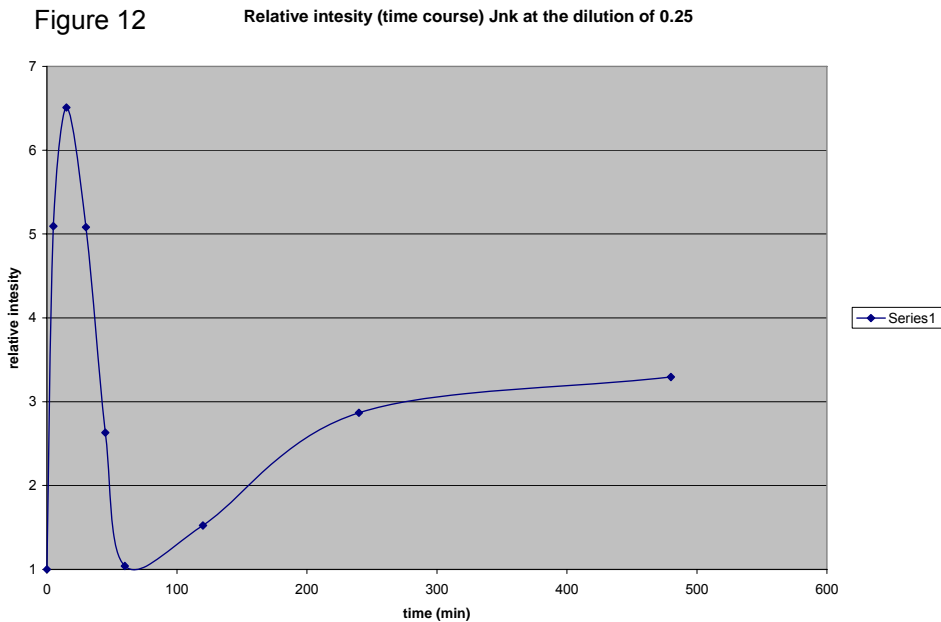


Figure 11 Relative intensity (time course) NF κ B at the dilution of 0.25

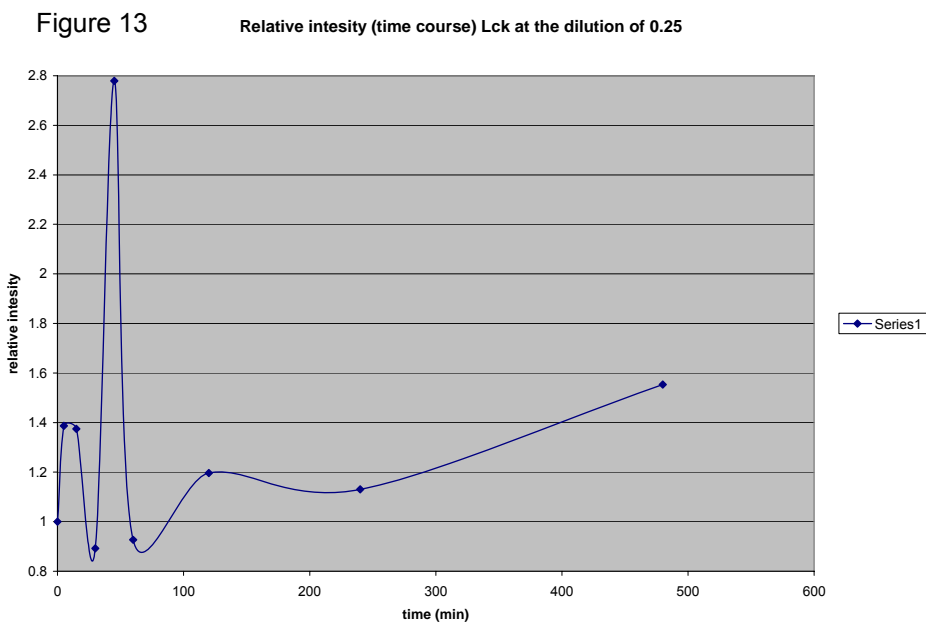


JNK (Figure 12) has been identified as a possible target with which *Francisella* interferes. We see an up regulation of JNK phosphorylation during first 5 and 15 minutes of infection, followed by a steady decrease until 60 minutes after which there is a slow up regulation until it reaches what appears to be a steady state. JNK normally suppresses BCL-2

signaling. This suppression may delay the apoptotic signaling cascade. Additional RPMA experiments and Western Blots will be performed in Year 2 to confirm these findings.



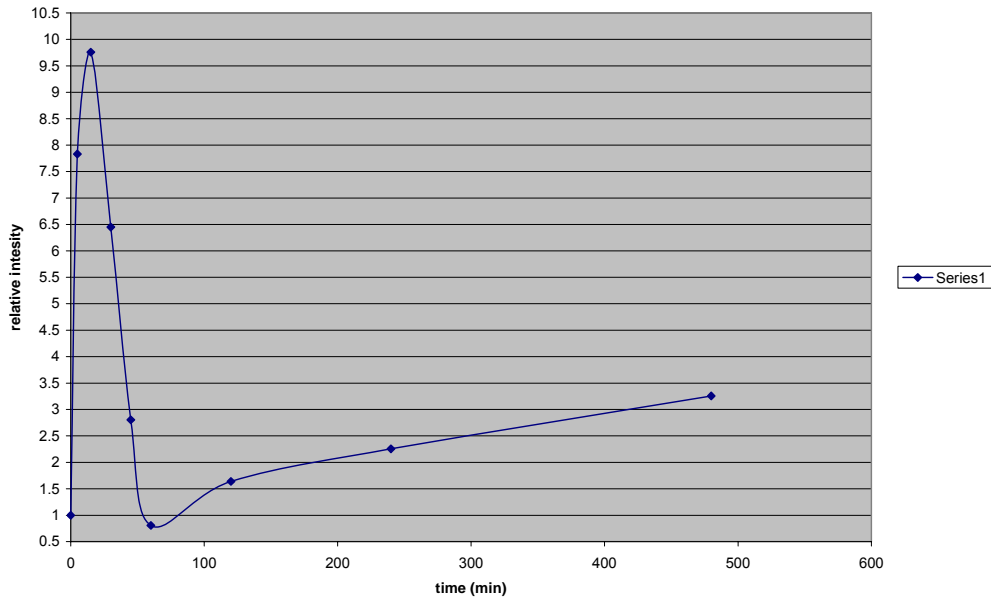
Lck (Figure 13) is generally associated with T cell activation; however in macrophages it can be activated during IL-2 receptor stimulation and further increase IL-2 production. This in turn leads to an adaptive immune response which stimulates T cells. Lck has recently been shown to be associated with AKT pathway, although its function is not fully understood. Another explanation could be that the cell is attempting to produce IL-2 in the presence of *Francisella*. However, it appears that whatever function Lck performs is being suppressed or inactivated through its interaction with *Francisella*. Additional RPMA experiments and Western Blots will be performed in Year 2 to confirm these findings.



The MAPK p38 (Figure 14) is involved in a number of different cell signaling events

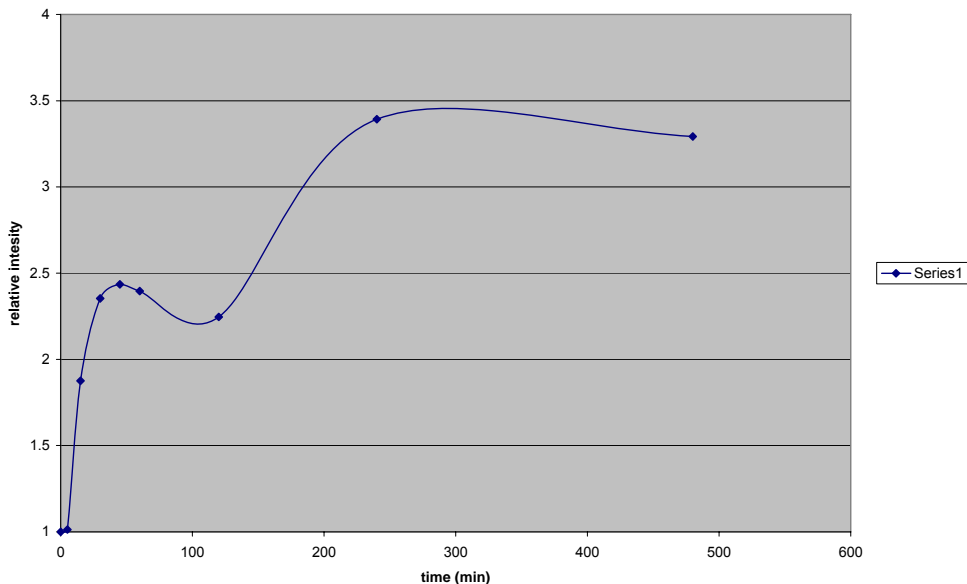
including the production of pro-inflammatory cytokines and apoptosis. Up regulation of p38 is seen during the first 15 minutes of the infection, followed by a decrease and eventual stabilization. This could indicate that early in the infection p38 is not blocked by *Francisella*; however as the infection progresses suppression of p38 occurs, resulting in a lack of cytokine production and apoptosis. Additional RPMA experiments and Western Blots will be performed in Year 2 to confirm these findings.

Figure 14 Relative intensity (time course) p38 at the dilution of 0.25



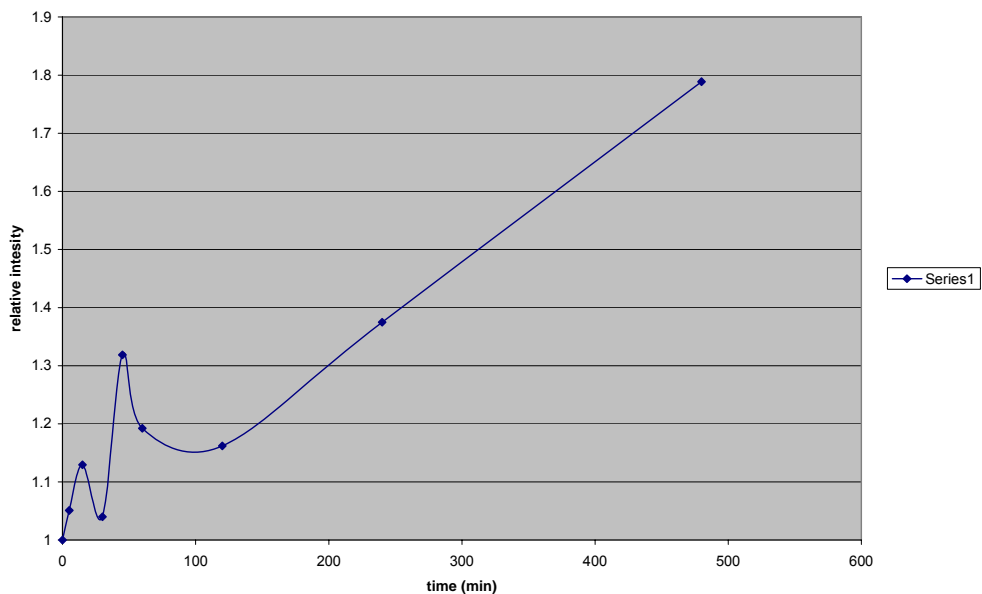
Src (Figure 15) is involved in cell cycle, activation of Mek/Erk pathway and also in making clathrin pits. A recent study showed after *Francisella* escapes from the phagosome and replicates in the cytosol it reenters an endocytic compartment via a trafficking event. Src demonstrated an overall up regulation during *Francisella* infection. It is possible that the early up regulation events are due to cell cycle arrest, whereas the latter events were associated with the production of this endocytic compartment. Additional RPMA experiments and Western Blots will be performed in Year 2 to confirm these findings.

Figure 15 Relative intensity (time course) Src at the dilution of 0.25



Bax (Figure 16) is positively expressed during apoptosis, and is considered pro-apoptotic. Here Bax has a gradual up regulated trend throughout the course of the infection experiment. This could indicate that during the later stage of *Francisella* infection when it is ready to leave the cell that Bax is needed to induce an apoptotic event. Additional RPMA experiments and Western Blots will be performed in Year 2 to confirm these findings.

Figure 16 Relative intensity (time course) Bax at the dilution of 0.25

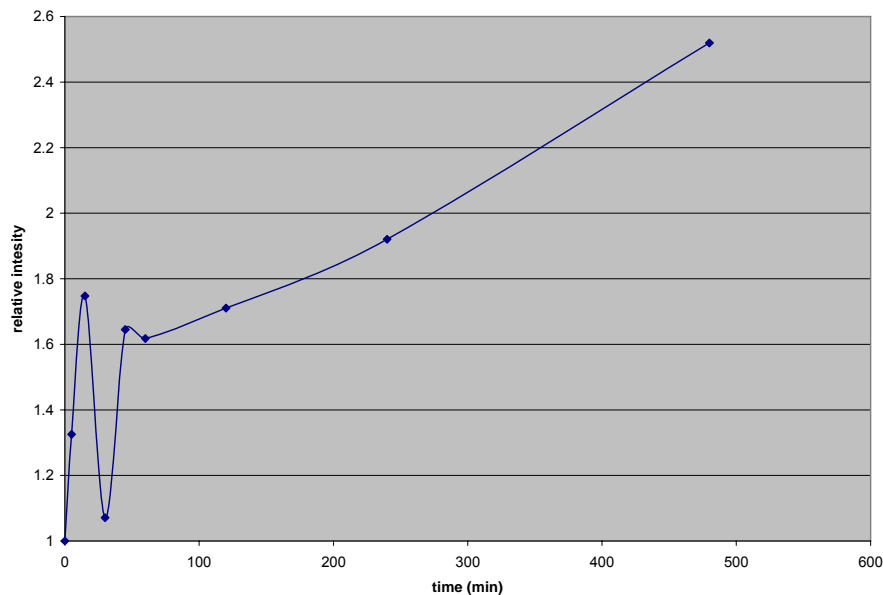


Bcl-2 (Figure 17) negatively regulates Bax, and is considered to be anti-apoptotic. It has the effect of being anti-apoptotic. Interestingly, the Bcl-2 activation pattern appears to mimic that of Bax. It is possible that *Francisella* causes up regulation of Bcl-2 in order to suppress Bax, until apoptosis is inevitable. Additional RPMA experiments and Western Blots will be performed in

Year 2 to confirm these findings.

Figure 17

Relative intensity (time course) Bcl at the dilution of 0.25



Task 1.4: Generate the phosphoactivation map of *Francisella* LVS infected human activated THP-1 (macrophage) cells. Compare the phosphoactivation profiles between J774A.1 and THP-1 cells. Provide conclusions regarding the differences in response of human and mouse cells to *Francisella* LVS infection.

Work on this task will begin in Year 2.

Task 1.5: Generate the phosphoactivation map of *Francisella tularensis* B38 infected J774A.1 macrophage cells. Compare the phosphoactivation profiles generated to published results with other *Francisella* strains in J774A.1 cells for validation.

Francisella tularensis B-38 strain was obtained from BEI Resources (ATCC) to ensure the consistency with the banked strains. Infection time courses have been prepared with J774A.1 with *Francisella* B38 and RPMA will be performed as soon as slides are available from the manufacturer.

Task 1.6: Analyze and compare the phosphoactivation profiles generated by the type strain B38 to vaccine (LVS) strain. Provide conclusions regarding the differences between the strains of *Francisella*.

Work on this task will begin in Year 2.

Task 1.7: Discussed before Task 1.1.

Task 1.8: Analyze and compare the phosphoactivation profiles generated by *F. novicida* to vaccine (LVS) strain. Provide conclusions regarding the differences between the strains of *Francisella*.

Work on this task will begin in Year 2.

Task 2: Screening of *Francisella* ORFs for potential VFs as a model for high-throughput screening of ORFs.

Task 2.1: Clone and express a set of *Francisella* proteins, including *F. tularensis*, *F. novicida* and *F. tularensis* LVS genes as available (and where they are significantly different than the *Ft* genes). Confirm activities (if known) of expressed proteins vs. native purified proteins.

In addressing Task 2, we began the process of cloning two of the selected potential *Francisella* virulence factors that will be used to test the scientific hypothesis. The Gateway (Invitrogen Corp, Carlsbad, CA) cloning Strategy for potential virulence factors was developed, and all the required Gateway cloning components were ordered.

Task 2.1.A: Cloning of 23 kDa protein, iglC:

Figure 18: PCR amplification of iglC gene. For cloning of the iglC gene (14, 15), genomic DNA was extracted from *F. novicida* using a genomic DNA purification kit (Promega Corporation). The primers were based on the sequence of the IGL-C gene in *F. novicida* (AY293576) and designed according to the manufacturer's manual for Gateway cloning (Invitrogen). The primers used are listed in Table 1. PCR was carried out in a PTC-100 Programmable Thermal Controller (MJ Research, Inc) using 50 ng of total DNA, 0.2 μ M of each primer, 0.2mM of each dNTP, 1.0 unit of Platinum® *Taq* DNA Polymerase High Fidelity (Invitrogen, Inc.), 2mM MgSO₄, and 1X High Fidelity PCR Buffer in a total volume of 50 μ l. The PCR amplification was performed using 40 cycles of 94°C for 30s, 70°C for 30s and 68°C for 1 min. The PCR product was cloned into pDONR221 vector (Invitrogen Inc.) and sequenced by Retrogen Inc. The arrow points to the iglC PCR fragment.

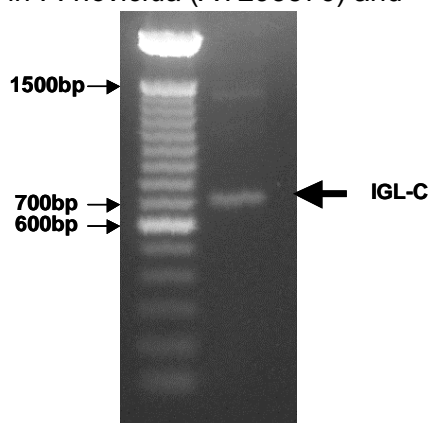


Table 1: IglC PCR primers for cloning into Gateway vectors

Primer	Sequence
Forward	5'-GGG GAC AAG TTT GTA CAA AAA AGC AGG CTA CCA TGG TGA TTA TGA GTG AGA TGA TA-3'
Reverse	5'-GGG GAC CAC TTT GTA CAA GAA AGC TGG GTC GTA TGC AGC TGC AAT ATA TCC-3'

Sequencing of the iglC in p-DONR221 revealed that the insert is present and in frame in the Gateway entry vector. The sequence is shown in **Figure 19** illustrating the Vector sequence and the iglC insert.

Figure 19: Sequencing results of igLC (in grey highlight) cloned into the Gateway entry Vector pDONR221 (in regular text).

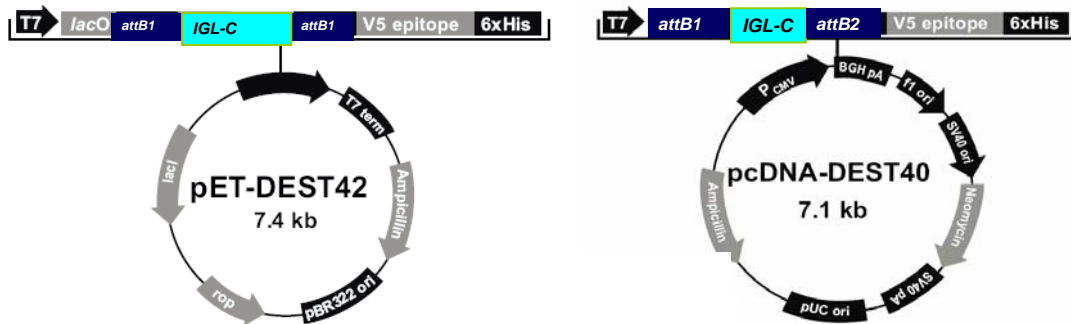
```

NCNGGCCCCAAATAATGATTTTATTTTGACTGATAGTGACCTGTTTCGTTGCAACAAATTGATGAGCAATGCTTTTTTA
T AATGCCAACTTTGTACAAAAAGCAGGCT ACC ATG GTG ATT ATG AGT GAG ATG ATA ACA AGA
CAA CAG GTA ACA AGT GGC GAG ACC ATT CAT GTG AGA ACT GAT CCT ACT GCA TGT ATA
GGA TCT CAT CCT AAT TGT AGA TTA TTT ATT GAT TCT TTA ACT ATA GCT GGG GAG AAA
CTT GAT AAA AAT ATC GTT GCT ATA GAG GGT GGA GAG GAT GTC ACG AAA GCT GAT TCG
GCT ACA GCT GCT GCT AGT GTA ATA CGT TTA TCT ATA ACG CCA GGC TCT ATA AAT CCA
ACA ATA AGT ATT ACT CTT GGT GTT CTA ATT AAA TCA AAT GTC AGA ACT AAA ATT GAA
GAG AAA GTT TCG AGC ATA TTA CAA GCA AGT GCT ACA GAT ATG AAA ATT AAG TTA GGT
AAT TCT AAT AAA AAA CAA GAG TAC AAA ACT GAT GAA GCA TGG GGT ATT ATG ATA GAT
CTA TCT AAT TTA GAG TTA TAT CCA ATA AGT GCT AAG GCT TTT AGT ATT AGT ATA GAG
CCA ACA GAA CTT ATG GGT GTT TCA AAA GAT GGA ATG AGT TAT CAT ATT ATA TCT ATA
GAT GGT CTT ACA ACA TCT CAA GGA AGC TTG CCA GTA TGT TGC GCA GCT AGC ACA GAT
AAA GGA GTT GCT AAA ATA GGA TAT ATT GCA GCT GCA TAC GAC CCA GCT TTC TTG TAC
AAA GTT GGC ATTATAAGAAAGCATTGCTTATC ATTTGTTGCAACGAACANGGTCACATCAGTCAAATAAAA

```

Following this successful insertion of our virulence factor gene into the central Gateway compatible vector, we performed the Gateway recombination reactions to obtain two additional vectors, one for Bacterial expression of the virulence factor gene for further purification and extracellular application to mammalian cells, and one for intracellular mammalian expression, to directly observe the effects of the bacterial virulence factor on the host cell phosphoproteome. The two C-terminal tagged constructs are illustrated in **Figure 20**.

Figure 20: C-terminal tagged IGL-C in Bacterial Expression Vector (a) and IGL-C in pcDNA-DEST Gateway Vector (Mammalian Vector) (b)



Task 2.1.B: Cloning of AcpA, acid phosphatase:

Genomic DNA from *Francisella novicida* was obtained using the Wizard genomic DNA preparation kit (Promega, Madison, WI) (**Figure 21**) and was used as template for PCR reaction. The primers were designed to clone the *Francisella novicida* gene AcpA into the Invitrogen Prokaryotic expression vector, pBAD/D-TOPO (Invitrogen, Carlsbad, CA) are listed in **Table 2**.

Table 2: AcpA PCR primers for cloning into pBAD-TOPO

Primer	Properties	Sequence
Forward	29mer, 34% GC, T _m 58	CACCAAGCTCAATAAAATTACCTTTAGGA
Reverse	33mer, 33%GC, T _m 58	GTTTAATTTATCCATCACTAATCCTGTCTTAGG

These primers will generate an insert of 1656 bp for cloning into the pBAD102/D-TOPO vector for a total plasmid size of 6017 bp. Genomic bacterial DNA was prepared from *Francisella* species and used as the starting material for the PCR reaction. The expression product including the Thioredoxin and His tag was a total of 2010 bp and has a calculated mass of 71 kDa. Following Enterokinase cleavage to remove the Thioredoxin moiety, the His-tagged recombinant protein will be 58.2 kDa. This protein will be expressed in *E. coli* and purified using Talon™ resin charged with Co²⁺. Purification will be confirmed by SDS-PAGE with coomassie blue staining. This gene has been cloned previously, so we anticipate that it should be fairly straightforward. Also, our collaborators have used the pBAD expression system to successfully clone and express other proteins. This strategy will allow the expression of tagged, recombinant AcpA which will be applied externally to cells prior to testing for RPMA effects. This cloning strategy was used to attempt to overcome prior difficulties that we experienced in attempting to clone this protein. In addition, we will reclone AcpA into the Gateway system for easier manipulation.

Figure 21: The isolated *F. novicida* and *F. philomiragia* genomic DNA was tested by gel electrophoresis. Lane one contains the standard molecular marker HyperLadder I. *F. novicida* DNA was in line five and *F. philomiragia* DNA was in lane six. Both samples of DNA were over 10,000 base pairs (bp) long. *Francisella* genomic DNA is about 1.9 million base pairs.

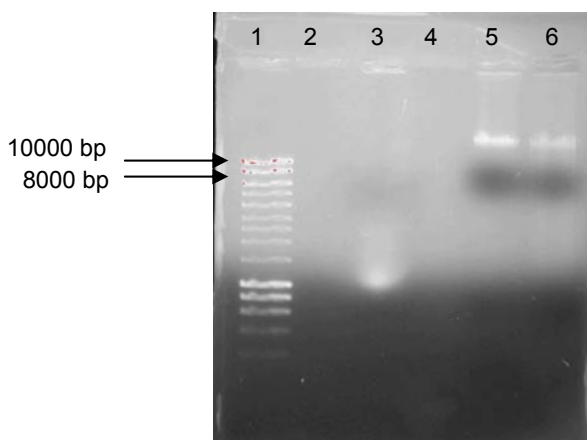
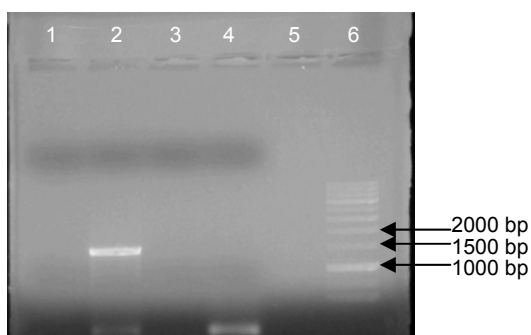


Figure 22: One microliter of genomic DNA from *F. novicida* and *F. philomiragia* were each tested with two different DNA polymerases (Taq and Pfx). Lane six consisted of the standard which was the molecular marker HyperLadder III. Lanes one and three had PCR product from DNA Taq polymerase, and it resulted in no PCR product. Lane 4 contained *F. philomiragia* DNA amplified with Pfx DNA polymerase which had a PCR product that was too small to be the Acid Phosphatase A gene. Lane two contained *F. novicida* DNA and Pfx DNA polymerase. Lane 2 had a PCR product that was about 1,700 base pairs which is the size of the cloned Acid Phosphatase A gene.



Task 2.1.C: Confirm Activity of expressed protein:

Task 2.1 states in part “Confirm activities (if known) of expressed proteins vs. native purified proteins.” The activity of iglC is unknown, although it is required for intracellular growth and replication and its expression is strongly upregulated upon intracellular infection by *Francisella* (Golovliov *et al.*, 1997). IglC is one of the approximately 30% of *Francisella* genes which have no homologies in the existing databases, and no obvious enzymatic activities or identifiable domains. Our working hypothesis is that this protein may be acting as a scaffold and forming complexes of proteins (bacterial and/or host) which may promote some function of intracellular bacterial growth. We will test this hypothesis by examining which host cell proteins (if any) may associate with the iglC protein when the iglC is immunoprecipitated following incubation with host-cell lysate, or when the iglC is expressed in mammalian host cells. We will identify associated proteins by subjecting the complex to LC-MS-MS. We feel that we have a unique opportunity with this technical approach to make an important contribution to the literature regarding potential binding partners of iglC and also demonstrating the power of the technologies (RPMA and LC-MS-MS) available to us through our collaboration with the proteomics group. The coupling of infectious disease research with the tools of proteomics will lead to many such exciting discoveries.

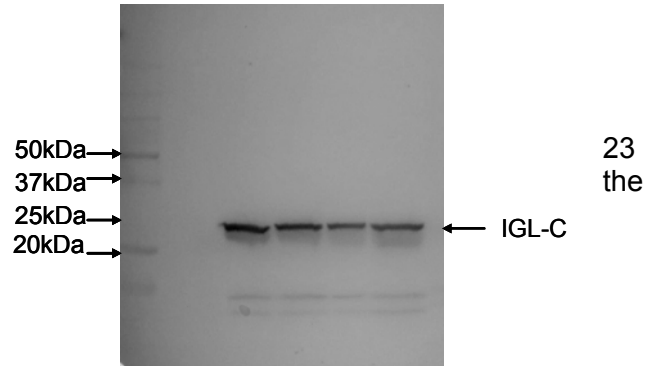
Task 2.2. Apply *Francisella* proteins extracellularly to mouse (J774A.1 macrophages) and human (activated THP-1) cells, then generate the phosphoactivation map.

Bacterial Expression of the iglC protein:

In order to move towards achieving the goals of **Task 2.2**, we plan to prepare purified tagged iglC protein using the bacterial construct described above. Purified iglC protein will be prepared, and can then be applied extracellularly to the mammalian cells and the response of those cells measured by RPMA analysis. **Figure 23** illustrates that BL21 *E. coli* bacteria

transformed with the iglC-Gateway vector express a tagged protein of the correct molecular weight. The purification is underway. The entry vector contained the iglC insert as was confirmed by sequencing, and the bacterial expression of V5 tagged iglC protein in BL21 *E. coli* has been confirmed by Western Blotting. Thus, using the Gateway system to shuttle between vectors was successful.

Figure 23: BL-21 *E. coli* bacteria transformed with the IglC-Gateway vector express a V5 – tagged protein with the correct molecular weight, a little bigger than kDa, which is the size of iglC (23kDa), plus six-His tag and the V5 tag.

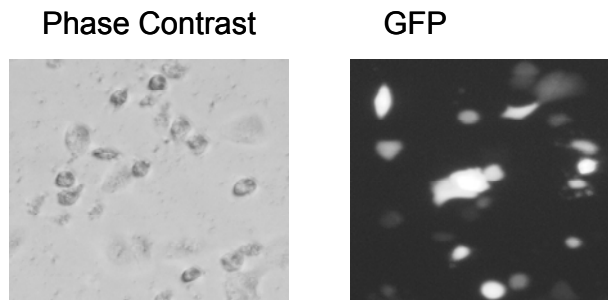


Task 2.3. Transfect plasmids expressing *Francisella* proteins into mouse (J774A.1 macrophages) and human (activated THP-1) cells, confirm intracellular expression, then generate the phosphoactivation map.

Mammalian Expression of the iglC gene:

Task 2.3 has been a technically challenging part of this quarters work. While we have easily observed bacterial expression of the iglC gene in bacteria using a bacterial expression vector (see above), we have had more difficulty in obtaining mammalian expression. We are concerned that the over-expression of iglC in J774A.1 macrophages may be harmful to the cells. Transfection efficiencies have been measured by the transfection of a GFP-expressing plasmid, and although there is some cell death as a result of the transfection itself, GFP expressing cells can be detected (**Figure 24**). However, the cells which were transfected with the iglC vector died and no live cells could be recovered after selection with 1.0 or 1.5 mg/ml G418.

Figure 24: Human lung epithelial cells (A549 cells) were plated to 6-well plate at 8×10^5 cells/well the night before transfection. Cells were then transfected with Lipofectamine 2000 (Invitrogen) according to the manufacture's instructions. pEGFP-C1 vector (Clontech) was used as transfection control. Transfection efficiency was checked under microscope 24 hours after transfection.



Previously, we reported having some trouble obtaining C-terminal tagged iglC expression using the Gateway Mammalian expression vector in the mammalian cells. In order

to solve this problem, we re-cloned iglC into the entry vector, and then into the N-terminal tagged Gateway Mammalian expression vector. The schematic for this vector is illustrated in **Figure 25**.

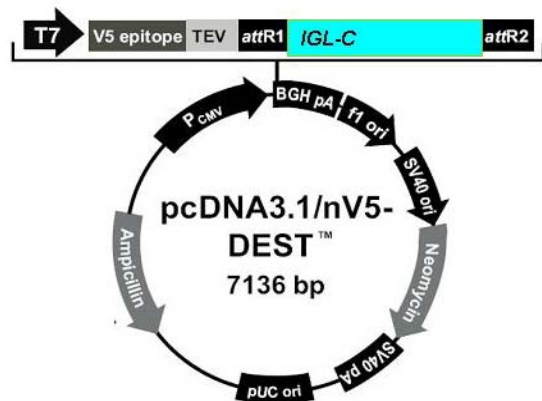
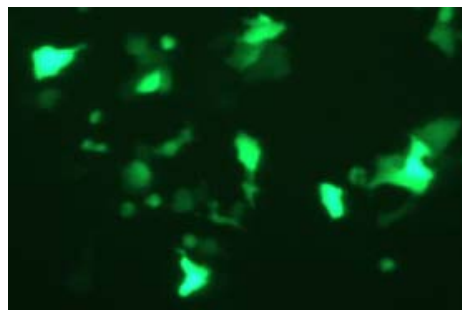


Figure 25: N-terminal tagged IGL-C in pcDNA-DEST Gateway Vector (Mammalian Vector).

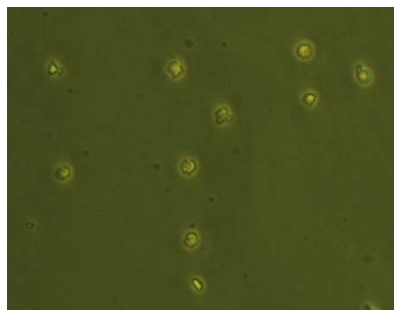
We used this construct to transfect the mammalian cells, and obtained selected cells. Human lung epithelium A549 cells were transfected with pcDNA 3.1/nV5-DEST-iglC and co-transfected with a GFP containing plasmid. Upon initial transfection, we observed approximately 30% of the cells were positive for GFP (Figure 26). Following 1 mg/ml G418 selection, all the non-transfected control cells were dead, and the pcDNA3.1-iglC transfected

cells were growing well. We are in the process of checking for N-terminal tagged iglC expression by RT-PCR, Western Blotting of whole cell lysate and immunoprecipitation using the anti-V5 tag antibody (Invitrogen, Carlsbad, CA).

Figure 26: A549 cells were plated in a 6-well cell culture plate the night before transfection. At the time of transfection, cells were about 80% confluent. Cells were transfected with Fugene 6 using a GFP vector as a control. The success of transfection was confirmed by taking a picture of the GFP control at 24 hours after transfection. Cells were then split and selected with 1.0mg/ml Geneticin. Six days after selection, all control cells are dead while the transfected cells are healthy.



GFP Transfection Control



Non-transfected cells



Transfected cells

Selected with 1.0mg/ml Geneticin

It may be that overexpression of this iglC bacterial virulence factor is harmful to mammalian cells. Such a finding, while disappointing, could confirm our choice of iglC as an important virulence factor of *Francisella*! If the N-terminal tagged iglC construct is not successfully expressed, our alternate approach is to move the iglC insert to a Gateway-compatible, inducible mammalian expression system, in which case we will be able to fully select for positive transformants without inducing the expression of the virulence factor gene,

igIC. Once transformants are obtained, expression of the cloned igIC gene can then be turned on, and the effects on the phosphoproteome measured.

KEY RESEARCH ACCOMPLISHMENTS:

- ✓ RPMA of *Francisella novicida* in J774A.1 murine macrophages
- ✓ RPMA analysis of the following proteins:
 - NFκB
 - IκBa
 - P38 MAPK
 - JNK
 - Src
 - Lck
 - Caspase 9
 - Caspase 3
 - Bcl2
 - Bax
- ✓ Comparison and correlation of RPMA results to published results of *Francisella* infection.
- ✓ Cloning of iglC protein, a known virulence factor of *Francisella*.
- ✓ Bacterial expression of tagged iglC protein.
- ✓ Mammalian expression of tagged iglC protein.

REPORTABLE OUTCOMES:

Monique L. van Hoek¹, Annie B. Verhoeven¹, SuHua Han¹, Yuka U. Taylor¹, Lance Liotta², Emmanuel Petricoin², Serguei Popov¹ and Charles Bailey¹. Phosphoproteome-based approach to the identification of bacterial virulence factors. 1. National Center for Biodefense and Infectious Diseases. 2. Center for Applied Proteomics and Molecular Medicine, Department of Molecular and Microbiology, George Mason University, 10910 University Boulevard, Manassas, VA 20110.

Poster prepared for Protein Kinase and Protein Phosphorylation FASEB Summer Research Conference, July 7-12, 2007.

CONCLUSION:

In the first year of this project, working on **Task 1**, we have successfully performed Reverse Phase MicroArray (RPMA) of *Francisella novicida* in J774A.1 murine macrophages. In so doing, we have performed detailed RPMA analysis of the following proteins over a time course of infection: NFkB, IKBa, p38 MAPK, JNK, Src, Lck, Caspase 9, Caspase 3, Bcl2, and Bax, among others. We present data illustrating time-specific changes in these proteins during infection representing the Toll-like receptor pathway, the AKT pathway and the apoptotic pathway. We have begun a comparison and correlation of RPMA results to published results of the effects of *Francisella* infection on host cells, the results of which will be presented in a poster and are being prepared as a manuscript from this work. We are beginning to generate a phosphoproteome map of the host cell response to *Francisella* infection.

We have also made significant progress on **Task 2**, including cloning of iglC and AcpA proteins, two known virulence factors of *Francisella* to be used in testing our hypothesis. We have successfully expressed tagged iglC protein in a bacterial expression vector and are purifying this protein for further study. In addition, we have confirmed by RT-PCR the mammalian expression of tagged iglC protein.

“So What”: We have demonstrated that RPMA can be used to rapidly characterize the effect of bacterial infection on host cells by examining alterations in phosphorylation of multiple signaling pathway proteins. Through the ability of the protein array technology to concomitantly measure hundreds of signaling events at once, in effect providing a real-time molecular network map, RPMA analysis will allow us to discover the full complement of signaling systems that could serve as new targets for rational intervention and therapy. The comparative analysis of signaling profiles will further aid us in understanding the key elements of virulence and pathogenesis, a critical step along the path to development of vaccines and therapeutics.

REFERENCES:

1. **Andersson, H., B. Hartmanova, P. Ryden, L. Noppa, L. Naslund, and A. Sjostedt.** 2006. A microarray analysis of the murine macrophage response to infection with *Francisella tularensis* LVS. *J Med Microbiol* **55**:1023-33.
2. **Checroun, C., T. D. Wehrly, E. R. Fischer, S. F. Hayes, and J. Celli.** 2006. Autophagy-mediated reentry of *Francisella tularensis* into the endocytic compartment after cytoplasmic replication. *Proc Natl Acad Sci U S A* **103**:14578-83.
3. **Duenas, A., M. Aceves, A. Orduna, R. Diaz, M. S. Crespo, and C. Garcia-Rodriguez.** 2006. *Francisella tularensis* LPS induces the production of cytokines in human monocytes and signals via Toll-like receptor 4 with much lower potency than *E.coli* LPS. *Int Immunol* **18**:785-795.
4. **Espina, V., E. C. Woodhouse, J. Wulfkuhle, H. D. Asmussen, E. F. Petricoin, 3rd, and L. A. Liotta.** 2004. Protein microarray detection strategies: focus on direct detection technologies. *J Immunol Methods* **290**:121-33.
5. **Fuller, C. L., K. C. Brittingham, M. K. Hepburn, J. W. Martin, P. L. Petitt, P. Pittman, and S. Bavari.** 2006. Dominance of human innate immune responses in primary *Francisella tularensis* live vaccine strain vaccination. *J Allergy clin immunol*:1186-1188.
6. **Hawlish, H., and J. Kohl.** 2006. Complement and Toll-like receptors: key regulators of adaptive immune responses. *Mol Immunol* **43**:13-21.
7. **Hrstka, R., J. Stulik, and B. Vojtesek.** 2005. The role of MAPK signal pathways during

- Francisella tularensis* LVS infection-induced apoptosis in murine macrophages. *Microbes Infect* **7**:619-25.
8. **Lai, X. H., I. Golovliov, and A. Sjostedt.** 2004. Expression of IgIC is necessary for intracellular growth and induction of apoptosis in murine macrophages by *Francisella tularensis*. *Microb Pathog* **37**:225-30.
 9. **Latz, E., and D. T. Golenbock.** 2003. Receptor "cross talk" in innate immunity. *J Clin Invest* **112**:1136-7.
 10. **Liotta, L. A., V. Espina, A. I. Mehta, V. Calvert, K. Rosenblatt, D. Geho, P. J. Munson, L. Young, J. Wulfkuhle, and E. F. Petricoin, 3rd.** 2003. Protein microarrays: meeting analytical challenges for clinical applications. *Cancer Cell* **3**:317-25.
 11. **Oda, K., and H. Kitano.** 2006. A comprehensive map of the toll-like receptor signaling network. *Mol Syst Biol* **2**:2006 0015.
 12. **Paweletz, C. P., L. Charboneau, V. E. Bichsel, N. L. Simone, T. Chen, J. W. Gillespie, M. R. Emmert-Buck, M. J. Roth, I. E. Petricoin, and L. A. Liotta.** 2001. Reverse phase protein microarrays which capture disease progression show activation of pro-survival pathways at the cancer invasion front. *Oncogene* **20**:1981-9.
 13. **Rajaram, M. V., L. P. Ganesan, K. V. Parsa, J. P. Butchar, J. S. Gunn, and S. Tridandapani.** 2006. Akt/Protein kinase B modulates macrophage inflammatory response to *Francisella* infection and confers a survival advantage in mice. *J Immunol* **177**:6317-24.
 14. **Telepnev, M., I. Golovliov, T. Grundstrom, A. Tarnvik, and A. Sjostedt.** 2003. *Francisella tularensis* inhibits Toll-like receptor-mediated activation of intracellular signalling and secretion of TNF-alpha and IL-1 from murine macrophages. *Cell Microbiol* **5**:41-51.
 15. **Telepnev, M., I. Golovliov, and A. Sjostedt.** 2005. *Francisella tularensis* LVS initially activates but subsequently down-regulates intracellular signaling and cytokine secretion in mouse monocytic and human peripheral blood mononuclear cells. *microbial pathogenesis* **38**:239-247.
 16. **Twine, S. M., Mykytezuk, M. D. Petit, H. Shen, A. Sjostedt, J. W. Conlan, and J. F. Kelly.** 2006. In vivo proteomic analysis of the interacellular bacterial pathogen. *Francisella tularensis*, isolated from mouse spleen. *Biochemical and Biophysical Research Communications* **345**:1621-1633.
 17. **Weng, M., and W. A. Walker.** 2006. Bacterial Colonization, Probiotics, and Clinical Disease. *J Pediatr* **149**:S107-S114.

APPENDICES:

None

SUPPORTING DATA:

None